Michael de Wild*, Sebastian Dany, Christoph John and Felix Schuler

Smart 4D-printed implants and instruments

Programmed, stimuli-responsive NiTi tools

Abstract: Selective laser melting (SLM) was used to manufacture smart programmed structures with customized properties made of biocompatible NiTi shape-memory alloy. A series of helixes was produced with systematically varied SLM process parameters *Laser Exposure Time* and *Laser Power* in order to specifically change the thermo-mechanical material properties of the 3D-structures. This innovation opens up the possibility to adjust the NiTi phase transformation temperature during the manufacturing process. This controllable property determines which of the two crystallographic phases *martensite* or *austenite* is present at a certain operating temperature and allows the mechanical properties to be adjusted: *martensitic* devices are soft and pseudo-plastic due to the shape-memory effect, whereas *austenitic* structures are pseudo-elastic. In a further step, the SLM process parameters were locally varied within 4D-printed twin-helixes. As a result, the phases, respectively the mechanical properties of a single component were adjusted at different locations. The ratio of elastic to plastic deformation and the spring constant of the helix can be locally controlled. This allows, for example, the spatio-temporal programming of 3D-printed surgical instruments or implants that are stimuli-responsive.

Keywords: 4D-printing, smart tools, Selective Laser Melting, NiTi, transformation temperature.

https://doi.org/10.1515/cdbme-2020-3053

***Corresponding author: Michael de Wild**: University of Applied Sciences Northwestern Switzerland, FHNW, School of Life Sciences, Institute for Medical Engineering and Medical Informatics IM^2, Hofackerstrasse 30, CH-4132 Muttenz, Switzerland, michael.dewild@fhnw.ch
Sebastian Dany: University of Applied Sciences Northwestern Switzerland, FHNW, School of Life Sciences, Institute for Medical Engineering and Medical Informatics IM^2, Hofackerstrasse 30, CH-4132 Muttenz, Switzerland. Hochschule Hamm-Lippstadt, D-59063 Hamm, Germany
Christoph John: Department of Chemistry, University of Basel, Mattenstrasse 24a, CH-4058 Basel, Switzerland,
Felix Schuler: University of Applied Sciences Northwestern Switzerland, FHNW, School of Life Sciences, Institute for Medical Engineering and Medical Informatics IM^2, Hofackerstrasse 30, CH-4132 Muttenz, Switzerland

1 Introduction

In many medical technology areas, implants and instruments e.g. cardiovascular stents or dental drills used for root canal treatments, are made of NiTi alloy, which can exist in the two different phases *martensite* and *austenite* [1]. Depending on the exact Ni□Ti ratio, either the shape-memory properties (e.g. for self-locking clips) or the pseudo-elasticity (for extremely deformable devices) are used. It is already known that NiTi devices can be additively manufactured [2].Moreover, the characteristic phase transformation temperature is depending on the applied laser energy because the bulk composition is enriched in Ti due to the higher vapour pressure of Ni compared to Ti [3] which shifts the transformation temperature to higher values. In this study we want to demonstrate that the thermo-mechanical properties of a twinned helix-device can be adjusted across different zones in a controlled manner. This extra dimension of programmed thermal-response is also called *4D-printing*.

2 Material and methods

2.1 Sample design and manufacturing

Both geometries, single and twin-helixes, were designed in SolidWorks™ (Dassault Systèmes, France) and produced on a modified Selective Laser Melting (SLM) machine (Realizer, DMG Mori, Germany). Single helixes with 3.5 turns and a diameter ø15 mm, height $L_0 = 20$ mm and rod thickness of 1.5 mm (see Fig. 1a) were produced with seven different laser *Exposure Times* (*ET*) 25, 32, 40, 50, 64, 80 and 100 µs. Two integrated end plates are used to apply a defined force.

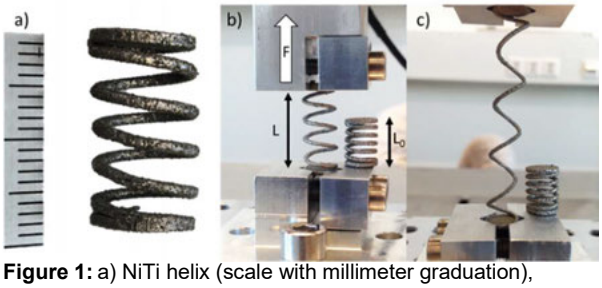

Figure 1: a) NiTi helix (scale with millimeter graduation), b, c) during tensile testing. A reference sample is next to it.

Furthermore, different *Laser Current* (*LC* [mA]) (*LC1600* and *LC2500*) were used on both sides of a twin-helix during SLM-production to program different transformation temperature into the material, see Fig. 2.

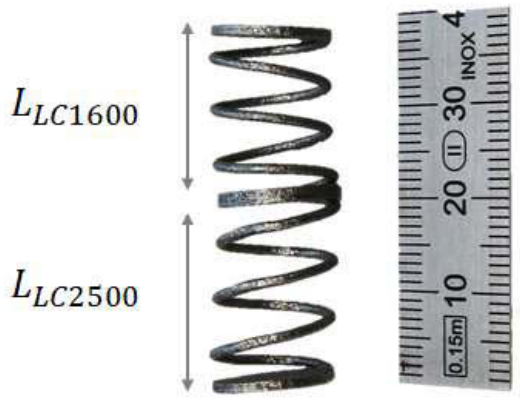

Figure 2: Smart twin-helix (L_0 = 40 mm, ø15 mm) produced using different SLM parameters *Laser Current* (*LC*).

2.2 Powder characterization

The particle size distribution of the starting NiTi powder [4] was determined by laser diffraction (Helos, with dry disperser RODOS and vibratory feeder, Sympatec GmbH, Clausthal-Zellerfeld, Germany) and the particle morphology was characterized by Scanning Electron Microscope (SEM, Hitachi TM3030Plus).

2.3 Differential scanning calorimetry

The transformation temperatures, e.g. A_f and A_p, of the starting powder, of all seven single helixes and of the two sides of the twin-helix were determined by Differential Scanning Calorimetry (DSC 214 *Polyma* NETZSCH, -150°C..150°C, 10 K/min).

2.4 X-ray diffractometry

A D2 Phaser XRD system in Bragg-Brentano geometry and LynxEye detector (Bruker, Karlsruhe, Germany, Cu-K_α X-ray radiation, λ = 1.5406 Å) was used to identify the crystallographic phases of monoclinic *martensite* B19' (PDF 00-35-1281, ICDD PDF2 powder diffraction data base, Philadelphia PA, USA) and cubic *austenite* B2 (PDF 01-076-3614) in *LC1600*- and *LC2500*-produced structures at room temperature. The diffraction measurements were carried out directly on the NiTi helixes in the 2□ angle range from 35° to 50° with a step size of 0.01° and an integration time of 2 s.

2.5 Tensile testing

The seven single helixes produced with different *ET* were mechanically characterized with a multipurpose servohydraulic testing system (Walter+Bai AG, Löhningen; Switzerland). Custom-made fixtures were used to clamp the end-plates of the samples at each end, see Fig. 1b. The tensile test was carried out by progressive loading/unloading cycles to determine the elastic and the plastic behaviour under pseudo-cyclic conditions. First, a preload of 1 N was applied at a speed of 0.5 mm/s to ensure defined contact conditions. The helix was then strained to 1 mm with a loading rate of 0.5 N/s. After the deformation *L* and the achieved force have been registered, the load was relieved and the shape-recovery of the first loading cycle was determined. In each subsequent loading cycle the helix was then iteratively elongated by an additional 1 mm and again relieved. Finally, after 33 loading cycles and a deformation of 33 mm, the experiment was stopped, see Fig. 1c.

2.6 Temperature-induced shape-recovery

The twin-helix with its two differently produces sides was immersed in liquid nitrogen for 2 minutes and cooled to -196°C. This is well below the *austenite* peak temperatures of both sides A_p^{LC1600} and A_p^{LC2500}, so that they both *martensitic*. The twin-helix was then compressed manually. In the cold state this (pseudo)plastic deformation remains, however, when heated later, will be reversed due to the well-known shape-memory effect. The cold, compressively deformed twin-helix was placed on a glass plate at room temperature and the warming-up and shape-recovery was observed using an IR camera (VarioCAM, Infratec AG). In addition, the temperature-induced shape-recovery was recorded using a visual camera. The resulting expansion of both sides of the twin-helix were quantified using a DIC video analysis software [5]. The corresponding transformation temperatures were derived from the thermograms.

3 Results

3.1 Powder characterization

The pre-alloyed NiTi powder particles exhibit spherical morphology (Fig. 3a) with a d_{50}-value of 57.2 ± 1.9 µm (see Fig. 3b) and an *austenite* finish temperature A_f = 24°C (see Fig. 4).

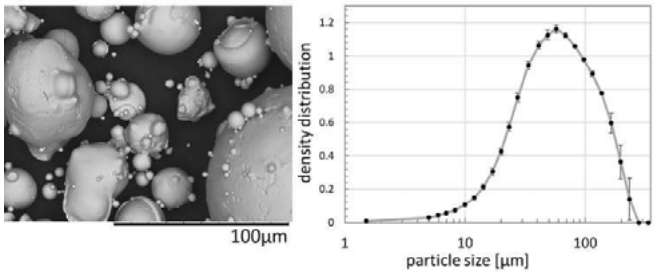

Figure 3: a) SEM image and b) particle size distribution of the starting NiTi powder (n = 3).

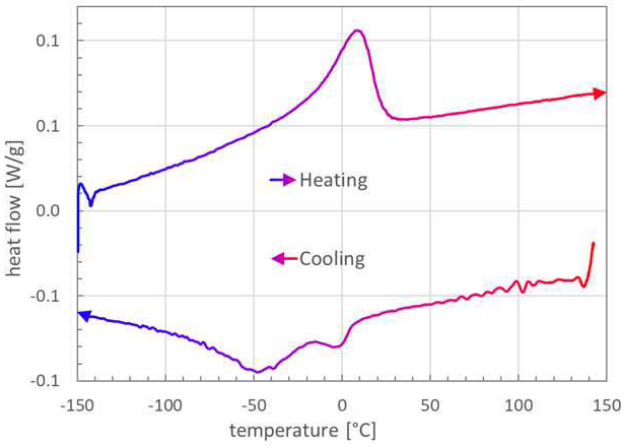

Figure 4: DSC curves of the starting NiTi powder.

3.2 Helix and twin-helix characterization

The produced NiTi single helix is shown in Fig. 1a. The SLM-process parameter-dependent phase transformation temperatures A_f of the seven samples in the series with varying laser *Exposure Time ET* are shown Fig. 7.

The twin-helix is shown in Fig. 2. DSC curves of material from both sides *LC1600* and *LC2500* are depicted in Fig. 5.

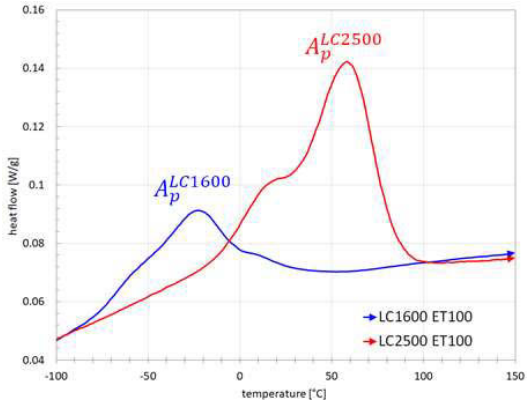

Figure 5: DSC hating curves from both sides of the twin-helix produced with specific SLM process parameters *Laser Current* (*LC*) *LC1600* and *LC2500*.

At room temperature the [111]-peak of the *martensitic* phase at 2□ = 44.92° can only be seen in the diffractogram of the *LC2500*-produced material. The *austenitic* [110]-peak at 2□ = 42.36° dominates on the *LC1600* side.

3.3 Tensile testing single helix series

The seven different helix samples *ET025* - *ET100* were mechanically investigated, see Fig. 1b and c: The progress of the spring deformation and the load maxima can be observed on the load curves (Fig. 6). The unloading curves of cycle 33 are also depicted. An elastic and a permanent plastic component can be clearly distinguished. The respective percentage of the elastic and plastic deformation are indicated in Fig. 7a. In addition, the spring constant, determined as the load-to-deformation ratio over the first 10 cycles, is plotted in Fig. 7b.

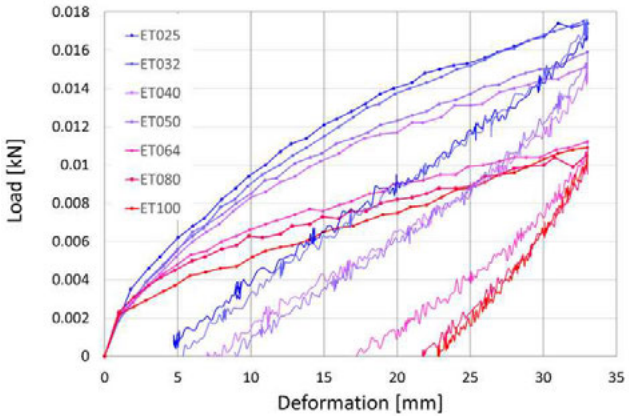

Figure 6: Loading and unloading curves of samples produced with specific SLM parameters *ET025* - *ET100*.

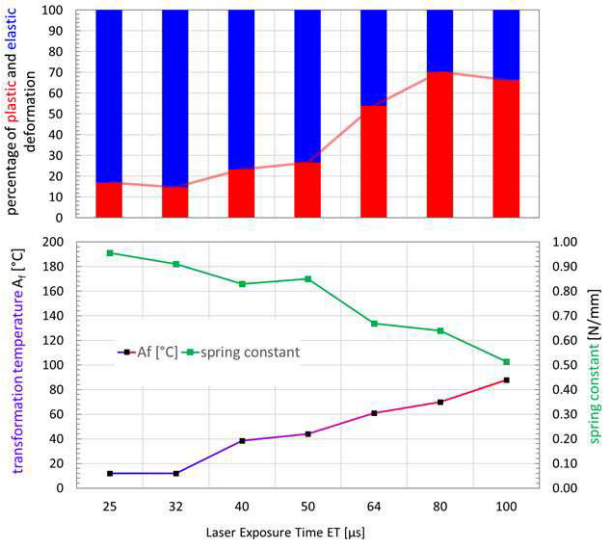

Figure 7: Mechanical properties of the samples *ET025* - *ET100*:
a) percentage of plastic and elastic deformation,
b) spring constant and **transformation temperature** A_f.

3.4 Temperature-induced shape-recovery of the twin-helix

Due to the cooling with LN_2 ($T_{LN_2} < A_p^{LC1600}, A_p^{LC2500}$) both sides of the compressed twin-helix are in the *martensitic* phase. The warming up and the shape-memory effect is shown in Fig. 8: While at -25°±10°C the upper part with the laser parameters *LC1600* already becomes *austenitic* and transforms back to its original geometry, the lower side *LC2500* initially remains in the deformed *martensite* (indicated blue). This side only returns to its original shape when it warms up to +45±10°C and also becomes *austenitic* (indicated red). These two transformation temperatures $T_{shape-recove}^{LC1600}$ and $T_{shape-recovery}^{LC2500}$, experimentally derived from thermograms during heating and shape-recovery, correspond well to the DSC-measured values, see Tab. 1.

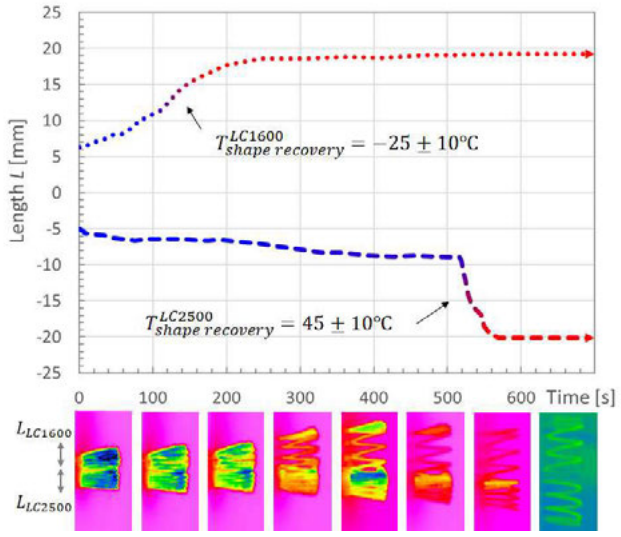

Figure 8: a) Temperature-induced shape-recovery and shape-memory phase transformation from *martensite* to *austenite* during warming up. b) Thermograms taken at different stages.

Table 1: Transformation temperatures A_p (from DSC, Fig. 5) and temperature of the observed shape-recovery $T_{shape\text{-}recovery}$ (from Fig. 8) at both sides of the twin-helix.

SLM parameter	A_p [°C]	$T_{shape\text{-}recovery}$ [°C]
ET100 LC1600	-23 ± 5	-25 ± 10
ET100 LC2500	58 ± 5	45 ± 10

4 Conclusions

We have demonstrated the possibility to locally adapt the thermo-mechanical properties of 3D components by zonally controlling SLM process parameters using a single starting powder. This 4D-printing technology allows, for example, the spatio-thermal programming of stimuli-responsive surgical instruments or implants. With this innovative approach new functionalities such as e.g. high damping elements, pseudo-elastic springs and shape-memory clamping-mechanisms could be combined in future devices.

Author Statement

Research funding: The SPIRITS project [6] is supported by the Region Grand Est, Land Baden-Württemberg, Land Rheinland-Pfalz, Cantons Baselstadt, Basellandschaft, Aargau, Swiss Confederation and by the program INTERREG Upper Rhine from the ERDF (European Regional Development Fund). Conflict of interest: Authors state no conflict of interest.

References

[1] ASTM F2063 – 18, *Standard Specification for Wrought Nickel-Titanium Shape Memory Alloys for Medical Devices and Surgical Implants*, ASTM International (2018).

[2] M. de Wild, F. Meier, T. Bormann, C.B.C. Howald, B. Müller, *Damping of selective-laser-melted NiTi for medical implants*, Journal of Materials Engineering and Performance, 23, 7; 2614-19 (2014).

[3] T. Bormann, B. Müller, M. Schinhammer, A. Kessler, P. Thalmann, M. de Wild, *Microstructure of selective laser melted nickel-titanium*, Materials Characterization, 94, 189-202 (2014).

[4] SAES Getters S.p.A., Viale Italia 77, I-20020 Lainate (Milan), Italy, https://www.saesgetters.com/

[5] Tracker, video analysis and modeling tool, https://physlets.org/tracker/

[6] INTERREG-project *Smart Printed Interactive Robots for Interventional Therapy and Surgery*, http://www.interreg-spirits.eu